Environmental Pollution 252 (2019) 1709–1718

Contents lists available at ScienceDirect

Environmental Pollution

journal homepage: www.elsevier.com/locate/envpol

Using scrap zero valent iron to replace dissolved iron in the Fenton process for textile wastewater treatment: Optimization and assessment of toxicity and biodegradability☆

Edison GilPavas [a], [*], Santiago Correa-Sánchez [a], Diego A. Acosta [b]

[a] GIPAB: Grupo de Investigación en Procesos Ambientales, Departamento de Ingeniería de Procesos, Universidad EAFIT, Cr 49 # 7 Sur 50, Medellín, Colombia
[b] Grupo de Desarrollo y Diseño de Procesos, Departamento de Ingeniería de Procesos, Universidad EAFIT, Carrera 49 No 7 sur-50, Medellín, Colombia

ARTICLE INFO

Article history:
Received 3 April 2019
Received in revised form
10 June 2019
Accepted 25 June 2019
Available online 28 June 2019

Keywords:
Industrial textile wastewater
Advanced treatment
Scrap zerovalent iron (SZVI)
H_2O_2
Optimization
Toxicity

ABSTRACT

A Fenton like advanced oxidation process (AOP) employing scrap zerovalent iron (SZVI) and hydrogen peroxide (H_2O_2) was studied for industrial textile wastewater treatment from a textile manufacturing plant located at Medellín, Colombia (South America). The wastewater effluent studied contains a mixture of organic compounds resistant to conventional treatments. The effect of initial pH and SZVI concentration and H_2O_2 concentration were studied by a response surface methodology (RSM) Box-Behnken design of experiment (BBD). The combined SZVI/H_2O_2 process led to reductions of 95% color, 76% of chemical oxygen demand (COD) and 71% of total organic carbon (TOC) at optimal operating conditions of $pH = 3$, $SZVI = 2000$ mg/L and $[H_2O_2] = 24.5$ mM. Molecular weight distribution measurement (MWD), ultraviolet–visible (UV–Vis) spectroscopy, HPLC, biodegradability and toxicity were used to characterize the pollutants after the treatment process finding that the resulting effluent was polluted mostly by low molecular weight carboxylic acids. A remarkable biodegradability enhancement of the effluent was evidenced by a BOD_5/COD ratio increase from 0.22 to 0.4; also, the SZVI/H_2O_2 process successfully reduced the toxicity from 60% to 20% of dead *A. Salina* crustaceans.

1. Introduction

Large amounts of industrial wastewater are discharged to the environment harming ecosystems and human life. Textile industry discharges polluted effluents that cannot be treated by conventional waste-water treatment processes (Donadelli et al., 2018; GilPavas et al., 2018). Because industrial textile wastewater (ITWW) has high contents of detergents, dyestuffs, additives, and other pollutants, it has low biodegradability and severe environmental impact because of the color generated by the azo-dyes it contains and their breakdown products that may be toxic and/or mutagenic (Gandhimathi and Thanga Ramesh, 2013).

Different pretreatment technologies for ITWW treatment have been broadly reported in literature, including Advanced Oxidation Processes (AOPs) (Badawy et al., 2009), which have been found to be effective for the removal of azo-dye organic pollutants (Donadelli et al., 2018; GilPavas et al., 2018). The Fenton process has been studied as a viable alternative for the treatment of wastewater containing several organic pollutants, but its major drawbacks are: (1) it is cost intensive, (2) its optimum operation pH is 3 and (3) it uses excessive amounts of ferrous ions. Therefore, alternatives such as zero valent iron (ZVI) assisted Fenton processes are of interest (Donadelli et al., 2018; Segura et al., 2015; Kallel et al., 2009).

ZVI-based processes involve several removal pathways including reduction and oxidation reactions (Keenan and Sedlak, 2008; Katsoyiannis et al., 2008) whose importance strongly depends on the nature of the target pollutant and the operating conditions (Katsoyiannis et al., 2008), such as pH, reagents' concentration, and reactor configuration (Donadelli et al., 2018). It has been reported that in a ZVI/O_2 system, dissolved O_2 (DO) is activated to produce reactive oxidant species (ROS). ROS nature is still unknown, but their production probably occurs in three stages: ZVI is oxidized, H_2O_2 and Fe^{2+} are formed, and ROS are generated through Fenton-like reactions. H_2O_2 is generated by adsorbed oxygen reduction on the surface of ZVI (Eq. (1)). Then, it can either be reduced by another electron transfer from ZVI (Eq. (2)), or react with Fe^{2+} into reactive oxidants such as hydroxyl radical •OH (Eq.

☆ This paper has been recommended for acceptance by Maria Cristina Fossi.
[*] Corresponding author.
E-mail address: egil@eafit.edu.co (E. GilPavas).

https://doi.org/10.1016/j.envpol.2019.06.104
0269-7491/

(3)) (Segura et al., 2015).

$$Fe^0 + O_2 + 2H^+ \rightarrow Fe^{2+} + H_2O_2 \quad (1)$$

$$Fe^0 + H_2O_2 + 2H^+ \rightarrow Fe^{2+} + 2H_2O \quad (2)$$

$$Fe^{2+} + H_2O_2 \rightarrow HO\bullet + OH^- + Fe^{3+} \quad (3)$$

As iron species are continuously released to the aqueous phase in ZVI-based processes, some studies have focused on the usage of batch systems with ZVI as source of iron cations in the presence of added H_2O_2 (ZVI/H_2O_2) for the degradation of azo dyes (Donadelli et al., 2018; Guo et al., 2015).

Although ZVI/H_2O_2 systems have been effectively applied for water treatment, only few studies have been conducted using actual industrial wastewater (Segura et al., 2015; Kallel et al., 2009). Most of the reported studies deal with synthetic effluents (Donadelli et al., 2018; He et al., 2012; Zhou et al., 2009). Moreover there are but a few studies that deal with real indigo dyeing effluents (Hendaoui et al., 2018; Olcay et al., 2014) and most of these studies have only dealt with the color removal of synthetic effluents containing indigo or indigo carmine dye (Bankole et al., 2017; Palma-goyes et al., 2014) and it is important to perform experimentation on real effluents because processes that were tested in synthetic dyed water might not work in a complex matrix such as the real effluent, on the other hand, characterization is important because the behavior of a real effluent is unpredictable, unlike the synthetic samples.

On the other hand, to the best of our knowledge, optimal operation conditions for COD and color degradation and monitoring of other parameters such as molecular weight distribution and toxicity have been scarcely reported, and these can provide a better understanding of the implications of the process when used for the treatment of ITWW. Nowadays, several researchers are conducting studies with scrap zerovalent iron (SZVI) for wastewater treatment (Kumar et al., 2012; Zhen et al., 2015) as this is a way to reutilize a byproduct from machinery industries. Also, SZVI has excellent reactivity, similar to that of ZVI, and at low cost. Therefore, by using SZVI as a replacement for ZVI treatment costs can be reduced, while also accomplishing reutilization of a waste material.

This research focuses on finding an economical and effective alternative for treating wastewater of the indigo dyeing and textile finishing processes of a local factory specialized in jeans manufacturing. This was done by the SZVI/H_2O_2 process, which was optimized by response surface methodology and design of experiment (BBD) to determine optimum operation conditions of pH, SZVI load and H_2O_2 concentration to minimize operational cost while keeping a viable enough COD and color degradation. Some parameters like toxicity, molecular weight distribution and analysis of intermediates by HPLC were monitored in the final effluent, which could be useful in future research to determine if it can be reused in other industrial process.

2. Experimental

2.1. Samples handling

Samples were gathered from a homogenization tank of a textile manufacturing plant at Medellin (Colombia). The color of the sample was blue due to the variety of pollutants and diversity of dyes used during the production process. Samples were kept refrigerated according to APHA's standard procedure to avoid compounds degradation (American Public Health Association (APHA), 2012).

2.2. Characterization techniques

The properties of the sample were measured by duplicate using a Spectronic Genesys 2 PC UV–vis spectrophotometer, absorbance was measured from 200 to 700 nm, in a quartz cell with a path of 1 cm. APHA's Standard methods were used for the analysis of chemical oxygen demand (method 5220D), total organic carbon (method 5310D), True Coloration (TC), BOD_5 (respirometric method 5210B), turbidity (method 2130B) and total solids (2540B) (American Public Health Association (APHA), 2012). H_2O_2 concentration was determined by spectrophotometry using titanium (IV) oxysulfate following DIN 38402H15. For H_2O_2 concentrations below 50 mg/L MQuant™ 110011 peroxide test was used. Generated carboxylic acids were identified and quantified by high-performance liquid chromatography (HPLC) using an Agilent 1200 Liquid Chromatography equipped with a Hi-Plex H, 300 mm 7.8 mm (i.d.) column, at 35 °C coupled with a photodiode array detector at $\lambda = 210$ nm. 20 μL aliquots were injected into the LC under the circulation of 4 mM H_2SO_4 at 0.6 mL/min as mobile phase (Garcia-segura et al., 2012).

2.3. Reagents

Deionized water with conductivity <1 μS/cm (Milli-Q, Massachusetts) was used to prepare the aqueous solutions. pH was controlled by adding sulfuric acid (H_2SO_4; Carlo Erba, purity = 96%) or dissolved sodium hydroxide pellets (NaOH; Sigma-aldrich) and hydrogen peroxide ($H_2O_{2,}$ = 30% w/w) was used for the SZVI/H_2O_2 experiments. Also, scrap SZVI (purity = 80.6%, measured by X-ray fluorescence with an Axios X-Ray Fluorescence Spectrometer, by wavelength dispersion) was collected from a local industry and was sieved to particle size of 600 μm. The scrap iron dust was washed in order to remove oxides and other impurities from the surface, with NaOH (4.5 M) for 30 min, then HCl (5 M) for 30 minutes, and 3 times with deionized water to remove residual ions. Residual H_2O_2 was quenched with MnO_2 (Sigma Aldrich; reagent grade ≥ 90%) to prevent interference during COD measurements.

2.4. ZVI/H_2O_2 treatment

Experiments were conducted in an open batch system. The system consisted of a 50 mL glass cylindrical reactor containing ITWW with a water-cooling jacket to keep the system at constant temperature at approximately 25 °C and a mechanical stirrer set at 400 rpm to keep SZVI suspended. H_2O_2 solution was then added to start the reaction and after 60 min, samples were centrifuged at 4000 rpm for 10 min and the supernatant was separated and analyzed. MnO_2 was used to prevent residual H_2O_2 from interfering in COD measurements. Duplicate measurements were performed for all runs. After completing each SZVI/H_2O_2 treatment, sample's COD and true coloration were measured and the removal percentages were calculated as shown in equations (4) and (5):

$$Color\ removal\ (\%) = \%DC = \left(\frac{C_0 - C_t}{C_0}\right)*100 \quad (4)$$

where: C_0 and C_t are the initial true color value (mg Pt-Co/L) and the true color at time t, respectively.

$$COD\ degradation(\%) = \%DCOD = \left(\frac{COD_0 - COD_t}{COD_0}\right)*100 \quad (5)$$

where: COD_0 is the initial COD value (ppm) and COD_t is the COD value at time *t*. All the experiments were conducted at an approximate temperature of 25 °C at 400 rpm agitation for all runs.

2.5. Operating cost

In order to analyze the economic convenience of the SZVI/H_2O_2 process, operating cost (OC) was calculated, including the H_2O_2 and H_2SO_4 consumption, as shown in equation (6). OC was then analyzed with a response surface methodology to determine the minimum cost that can be achieved while meeting legal constraints for effluents' discharge.

$$OC = \frac{\left(Q_{H_2SO_4}C_{H_2SO_4} + Q_{H_2O_2}C_{H_2O_2} + Q_{SZVI}C_{SZVI} + C_EQ_E + Q_SC_S\right)}{V} \quad (6)$$

where, C_{H2SO4} is the cost per kilogram of H_2SO_4 (0.1026 USD/kg H_2SO_4) and Q_{H2SO4} is the quantity (in kg) of H_2SO_4 needed to adjust the pH to achieve the desired conditions. C_{H2O2} is the cost of H_2O_2 (0.34 USD/L H_2O_2) and Q_{H2O2} is the amount (in L) of H_2O_2 used in the process. C_{SZVI} is the cost preparing a 1 kg of SZVI and Q_{SZVI} the necessary amount SZVI for the process. C_E is the overall cost of energy (mainly for agitation in the process) (For the Colombian market, in April 2019 the price of electrical energy for industrial sector was 0.19 USD/kW-h) and Q_E is the amount (in kW-h) of energy consumed in the process and C_S is the cost of treating the sludge (sludge disposal, including transportation and excluding drying costs, was 0.01 USD/kg) and *Qs* is the amount of sludge generated by the process (in kg) and *V* (m^3) is the reaction volume. These data correspond to the Colombian market and they were updated to the year 2019 (Legiscomex Business Intelligence System).

2.6. Experimental design and statistical analysis

A 3 factors Box-Behnken Design (BBD), was used to achieve the optimal reaction conditions of the SZVI/H_2O_2 process *(i.e., to maximize COD)*. The independent variables and their levels were determined according to the results of preliminary tests and previous works (Donadelli et al., 2018; Segura et al., 2015; Kallel et al., 2009): (i) SZVI load: 2000–10000 mg/L; (ii) H_2O_2 dosage: 4.9–24.5 mM; and (iii) pH: 3 and 9.

The response variable was fitted to a polynomial quadratic model as function of the variables (pH,SZVI, and H_2O_2) and their interactions; this model was then used to fit the response variables %DCOD, %DC and OC as in Eq. (7) (Montgomery, 2017), using R project Software. The model was then used to generate tridimensional response surface plots where individual factors, effects on each response variable are visualized.

$$Y_i = \beta_0 + \sum_1^3 \beta_i X_i + \sum_1^3 \beta_i X_i^2 + \sum_1^3 \sum_1^3 \beta_{ij} X_i X_j \quad (7)$$

where: β_0, β_i, β_{ii}, and β_{ij} are the regression coefficients for the intercept, linear, square, and interaction terms, respectively; and x_i and x_j are independent variables. Analysis of variance (ANOVA) and *p*-values were used to determine which factors had a significant effect on the response variables. The quadratic model was also used to determine the optimal operating conditions for the independent variables. The reported values correspond to the average of the measurements; variability is shown by error bars in the graphs.

2.7. Toxicity assessment

Acute toxicity tests were performed by duplicate before and after the treatment. The mortality of *A. Salina* when exposed to the sample was checked to determine the toxicity. *A. Salina* subjects were bred in a medium that fulfilled the conditions for the growth and survival of the subjects. Test containing twenty *A. Salina* in the presence of 9.5 mL of the sample and 0.5 mL of growth medium were incubated for 24 h at 25 °C and with surface illumination provided by a lamp (3500 Lux). No nourishment was provided to the subjects during the whole process. Immobilization was observed after 24 h incubation. The crustaceans were considered immobile if they remained still for 15 s of observation (da Costa Filho et al., 2016). Acute toxicity was calculated as the percentage of immobilized subjects compared to a nontoxic control. The mortality of *A. Salina* was calculated as follows:

$$Mortality(\%) = \left(\frac{N_0 - N_t}{N_0}\right)x100 \quad (8)$$

where, N_0 was the initial number of living *A. Salina* and N_t was the living number at time t.

2.8. Isolation and fractionation

Samples were divided by ultrafiltration into five fractions according to their Molecular Weight Distribution (MWD): (i) MW < 3 kDa, (ii) 3 < MW < 5 kDa (iii) 5 < MW < 10 kDa, (iv) 10 < MW < 30 kDa and (v) MW > 30 kDa. The membranes used were Ultracell regenerated cellulose, 44.5 mm, Millipore Corporation, (Germany), with MW cut-offs of 3 kDa, 5 kDa, 10 kDa and 30 kDa. Membranes were washed with 0.1 M NaOH for 30 min and flushed with deionized water before each usage and preserved in a 10% ethanol/water solution at 4 °C, according to the manufacturer's instructions. The ultrafiltration process was conducted in a 50 mL ultrafiltration system from Amicon® Stirred Cell, EMD Millipore-Merck, (Darmstadt, Germany) and the operational pressure of ultrafiltration was kept constant at 0.2 MPa by a steady supply of highly pure N_2 (99.999%). Raw wastewater and post process water was filtered through ultrafiltration membranes with different MW cut-offs. To avoid contamination due to membrane fouling, the initial 5 mL of filtrate from each ultrafiltration process was discarded. Afterward, the TOC concentration of each filtrate fraction was determined.

3. Results and discussion

3.1. ITWW sample characterization

ITWW characterization is presented in Table 1. The sample displayed an intense blue color because of the presence of the indigo dye, denoting a high content of organic compounds, which is also indicated by the values of COD and TOC. Also, it can be concluded that the effluent is not biodegradable as the BOD_5/COD ratio is 0.22 (<0.4) (GilPavas et al., 2017a).

3.2. SZVI/H_2O_2 process

SZVI/H_2O_2 process was used to reduce the organic matter load, which was measured by COD concentration and color; also, to increase biodegradability of the samples. A BBD was used to determine the statistical significance of the effects of the evaluated variables and their interactions on the response variables (%DCOD and %DC). The results of the experimental design are presented in Table 2. Notice that the COD removals between 17 and 55% were achieved with the process.

To optimize the SZVI/H_2O_2 operating conditions (i.e., to maximize COD degradation, %DC and to minimize OC), multivariate

Table 1
ITWW characterization before and after SZVI/H_2O_2 treatment; and efficiency at optimal operating conditions.

Parameter	ITWW	Emission limit[a]	SZVI/H_2O_2 Process	Treatment efficiency (%)
pH	9.1	6–9	6	–
Conductivity (mS/cm)	12.76	–	15.06	–
Turbidity (NTU)	569	–	6	98.6
COD (mg O_2/L)	875	400	208	76
TOC (mg O_2/L)	324		93	71
BOD_5 (mg O_2/L)	189.6	200	87.9	53.64
Absorbance (660 nm)	1.8	–	0.09	95
True Color (mg Pt/L)	1,366	–	121	91
ISO 7887:2012-04 (B,C)	$\lambda_{436} = 96$	–	$\lambda_{436} = 7.6$	92 (λ_{436})
λ = 436-525-620 m (m^{-1},B)	$\lambda_{525} = 83$		$\lambda_{525} = 5.4$	94 (λ_{525})
	$\lambda_{620} = 74$		$\lambda_{620} = 4.2$	94 (λ_{620})
BOD_5/COD	0.2167	0.4	0.4	–
Toxicity (% mortality *Artemia salina*)	60	–	20	67
Generated sludge (kg/m^3)	–	–	0.295	
Operating costs, (USD/m^3)		1.04		

[a] Emission limit values for the discharge of industrial wastewater sewer system according to 0631 Resolution of 17/03/2015, issued by the Ministry of Environment and Sustainable Development of Colombia (South America).

Table 2
Experimental results of the SZVI/H_2O_2 process for %DCOD, %DC and OC according to the BBD. Reaction time of 60 min.

Run	pH	SZVI (mg/L)*10^3	H_2O_2 (mM)	%DC		%DCOD		OC (USD/m^3)	pH_{final}
				Y_{exp}	Y_{pred}	Y_{exp}	Y_{pred}		
1	6	6	14.55	12.52	12.33	22.9	24.9	0.87	7.5
2	9	10	14.55	10.4	16.76	17	20.05	1.08	7.91
3	3	10	14.55	83.9	88.01	63.6	60.98	1.08	5.34
4	3	6	4.85	71	65.82	51.6	55.69	0.69	5.31
5	3	2	14.55	91	84.65	62.4	59.35	1.08	4.79
6	6	10	4.85	13.6	14.69	25.8	24.34	0.47	7.41
7	6	6	14.55	12.1	12.33	25.3	24.9	0.87	7.68
8	3	6	24.25	95.82	100	74.3	75.88	0.89	6.11
9	6	2	24.25	33.48	32.41	31.3	32.76	0.67	7.76
10	6	2	4.85	30.06	41.6	25.3	24.26	0.47	7.83
11	6	10	24.25	81.13	69.59	37.3	38.34	0.67	7.26
12	9	6	4.85	14.8	7.37	24.1	22.51	0.69	7.93
13	9	2	14.55	13.97	9.86	13.4	16.03	1.08	7.8
14	6	6	14.55	12.37	12.33	26.5	24.9	0.88	7.34
15	9	6	24.25	10.47	15.66	28.9	24.81	0.89	8.0

regression was used to adjust the data to the models presented in Eqs. (9) and (10). These empirical models allow the prediction of values for %DCOD and %DC as a function of the independent process variables (SZVI load, H_2O_2 concentration, and pH), respectively. Correlation coefficients of $R^2_{adj} = 90.7$ for %DC and $R^2_{adj} = 95.15$ for %DCOD show that the model predictions match the results accurately (Table 3).

$$\%DC = 234.37 - 39.59*pH - 16.69*SZVI - 3.73*[H_2O_2] + 2.55*pH^2 + 0.0735*pH*SZVI - 0.250*pH*[H_2O_2] + 0.907*SZVI^2 + 0.413*SZVI*[H_2O_2] + 0.135*[H_2O_2]^2 \tag{9}$$

$$\%DCOD = 117.24 - 24.42*pH - 0.2375*SZVI - 0.357*[H_2O_2] + 1.61*pH^2 + 0.05*pH*SZVI - 0.1538*pH*[H_2O_2] + 0.0188*SZVI^2 + 0.0354*SZVI*[H_2O_2] + 0.0566*[H_2O_2]^2 \tag{10}$$

Response surface plots were generated from Eqs. (9) and (10) to visualize the simultaneous effect of 2 variables in the %DCOD and %DC. pH and H_2O_2 were the most significant effects, so in order to visualize their behavior SZVI load was fixed to a value of 2000 mg/L (Fig. 1(a) and (b)). As it can be noticed higher doses of H_2O_2 and lower pH lead to the highest %DCOD but, according to Eq. (6), they also lead to higher operational costs. Thus, extreme values for said variables are not desirable. This agrees with the literature, where it is reported that acidic conditions favor the oxidative pathways that are more effective in the degradation of organic compounds than the reductive pathways favored by basic conditions (Donadelli et al., 2018).

3.3. Effect of H_2O_2 concentration

Since iron species are continuously released into the aqueous phase, H_2O_2 becomes a limiting reagent in the process. Therefore, higher doses of H_2O_2 reach higher %DCOD as they enhance the production of •OH radical. The highest removal efficiency was attained at 24.3 mM of H_2O_2 (Fig. 1 (a), (b) and (c)). In order to determine if further increase in H_2O_2 concentration would increase %DCOD, experimental runs with H_2O_2 concentration over 24.3 mM were performed (as shown in Fig. S1, Supplementary Material); %DCOD remained stable until approximately 34 mM, but started decreasing with higher doses (%DCOD = 65% at 40 mM). Above 24.3 mM, the oxidation rate decreases when H_2O_2 is increased. This is probably because of the auto-decomposition of H_2O_2 into O_2 and H_2O (Eq. (11)), and the scavenging of •OH by H_2O_2 (Eq. (12)) as follows;

$$2H_2O_2 \rightarrow 2H_2O + O_2 \tag{11}$$

$$HO^{\bullet} + H_2O_2 \rightarrow HO_2^{\bullet} + 2H_2O \tag{12}$$

Table 3
Analysis of Variance for %DC. %DCOD y OC as a function of initial pH, SZVI load and H_2O_2 concentration, reaction time of 60 min.

Factor (%DC)	Sum of squares	Degree of freedom	Mean square	*F* value	*P* value
X:pH	10663.8	1	10663.8	97.39	0.0002
Y:SZVI	52.6338	1	52.6338	0.48	0.5190
Z:H_2O_2	1045.16	1	1045.16	9.55	0.0272
XX	1948.35	1	1948.35	17.79	0.0083
XY	3.1152	1	3.1152	0.03	0.8727
XZ	212.43	1	212.43	1.94	0.2224
YY	778.05	1	778.05	7.11	0.0446
YZ	1027.52	1	1027.52	9.38	0.0280
ZZ	597.53	1	597.53	5.46	0.0667
Total error	547.48	5	109.5		
Total (corr.)	16480.9	14			
$R^2 = 96.68\%$ $R^2_{adj} = 90.70\%$					
Factor (%DCOD)	**Sum of squares**	**Degree of freedom**	**Mean square**	***F* value**	***P* value**
X:pH	3549.03	1	3549.03	211.27	0.0000
Y:SZVI	15.9613	1	15.9613	0.95	0.3744
Z: H_2O_2	253.13	1	253.13	15.07	0.0116
XX	776.31	1	776.31	46.21	0.0010
XY	1.44	1	1.44	0.09	0.7814
XZ	80.10	1	80.10	4.77	0.0807
YY	0.3323	1	0.3323	0.02	0.8936
YZ	7.56	1	7.56	0.45	0.5320
ZZ	104.70	1	104.70	6.33	0.0547
Total error	83.99	5	16.80		
Total (corr.)	4844.34	14			
$R^2 = 98.27\%$ $R^2_{adj} = 95.15\%$					
Factor OC($USD/$m^3$)	**Sum of squares**	**Degree of freedom**	**Mean square**	***F* value**	***P* value**
X:pH	0.0021	1	0.0021	0.4	0.5528
Y: SZVI	0.0093	1	0.0093	1.75	0.2435
Z: H_2O_2	0.045	1	0.0458	8.6	0.0325
XX	0.5918	1	0.5918	111.06	0.0001
XY	0.0350	1	0.035	6.57	0.0505
XZ	0.0125	1	0.0125	2.35	0.1858
YY	0.008	1	0.008	1.52	0.2728
YZ	0.0857	1	0.0857	16.08	0.0102
ZZ	0.1762	1	0.1762	33.08	0.0022
Total Error	0.0266	5	0.0053		
$R^2 = 97.44\%$ $R^2_{adj} = 92.85\%$					

Moreover, excess H_2O_2 may react with ferric ion (Fe^{3+}) to form weaker ROS like the hydroperoxyl radicals (HO_2•), which is less reactive than HO• towards COD removal (Kavitha & Palanivelu, 2005). Thus, excess of H_2O_2 will react with HO• competing with the organic degradation and reducing treatment's efficiency. This agrees with previous studies on the oxidation of organic matter in wastewaters (Kavitha & Palanivelu, 2004, 2005; Ghanbari & Moradi, 2015).

3.4. *Effect of initial pH*

pH is a very important variable which affects the %DC and %DCOD in the SZVI/H_2O_2 oxidation process. Chen et al. (2001) reported that the zero valent iron decolorization rate decreases when the pH is alkaline. At such pH, Fe^{2+} ions and hydroxyl ions may precipitate as ferrous hydroxide on the surface of SZVI occupying the reactive sites and interfering with the reaction. Also, Donadelli et al. (2018) (Donadelli et al., 2018) reported that alkaline pH favors the reductive pathways for the degradation of pollutants which are less efficient than the oxidative ones that are favored in acidic media. Additionally Cao et al. (1999) found that the degradation rate of dye polluted wastewater by the ZVI process is strongly dependent on the pH. They found that the degradation is enhanced with the decrease of pH. However, an extremely low pH condition would compromise the treatment cost. Furthermore, the strong corrosion of iron would increase the color of the sample, resulting in problems in the discharge. The effect of initial pH in SZVI process is shown in Fig. 1 ((a), (b)). It revealed that SZVI was more effective at a low pH. Maximum efficiencies of COD removal (75%–55%) were achieved in the lower pH levels, near a value of 3 (Fig. 1 (a)), the removal efficiencies significantly dropped at higher pH values around 5 and 9 (35 and 25% respectively).

Furthermore, pH suffered a major variation during SZVI/H_2O_2 process; it increased from 3 to 6.3 (Fig. 3 (a)) within the first 15 min of reaction, and remained constant afterwards (60 min, pH = 6.2). The pH increase was probably due to the formation of hydroxyde ions attributed to the reaction of SZVI's with water, as shown in Eq. (13) (He et al., 2012).

$$Fe^0 + H_2O \rightarrow Fe^{2+} + H_2 + 2HO^- \tag{13}$$

3.5. *Effect of SZVI dose*

Higher SZVI load provides more surface active sites that may increase rate of reaction resulting in more iron ions triggering the subsequent reactions, resulting in the degradation of dye molecules to remove color (Ming-Chin et al., 2006). However, excess concentration of Fe^{2+} can be a scavenger for HO• and attenuate the degradation (Masomboon et al., 2009). The effect of different SZVI dosages on COD removal efficiency is shown in Fig. 1 (c). The color and COD removal efficiency were enhanced with a higher dosage of SZVI. With a SZVI dosage of 2000, 6000 and 10000 mg/L, COD removal efficiency was 74, 76 and 78%, respectively, after 60 min reaction time. When the dosage of iron exceeded 2000 mg/L, COD removal scarcely increased. Although the effect of SZVI load was not significant, blank tests were performed to determine if the process

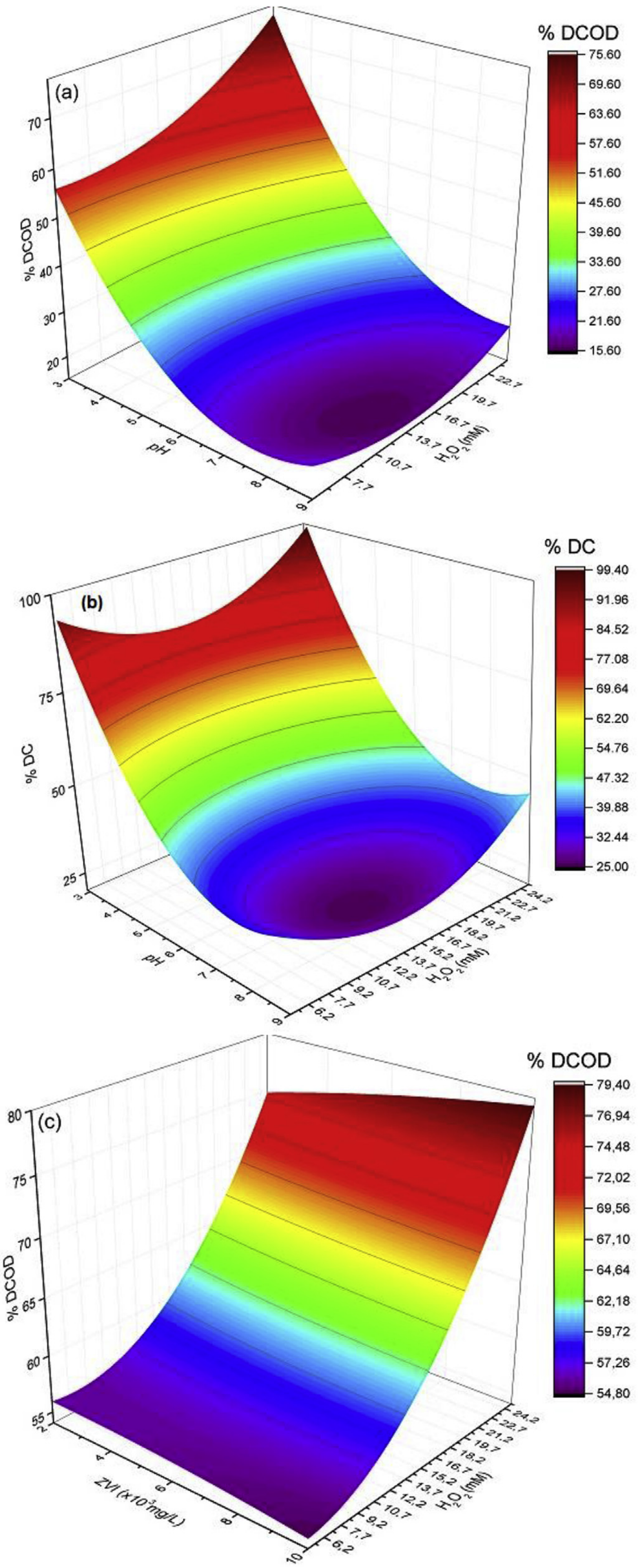

Fig. 1. Effect of pH and H_2O_2 and their interaction on %DCOD (a), %DC (b) with SZVI = 2000 mg/L; and the interactive effect of SZVI and H_2O_2 on %DCOD with pH = 3 (c) using a response surface diagrams.

would work without SZVI, only H_2O_2, this tests didn't exceed 26% of %DCOD; this agrees with previous studies which reported that although ZVI was necessary for the process to work properly, %DCOD would only increase with a higher load of SZVI until a certain concentration, but it would remain steady above it (Segura et al., 2015; Kallel et al., 2009).

At 60 min, COD removal efficiency stabilized around 78% for all ZVI doses. This leads to conclude that there is a transition in SZVI process between the iron dosage of 2000 and 10000 mg/L. Since excess amounts of iron could increase the mass transfer, and cause an overdose of Fe^{2+} that might react with the hydroxyl radicals and inhibit the reaction (Kallel et al., 2009), 2000 mg/L seems to be an appropriate dosage.

3.6. *Model validation*

In order to validate the capacity of the model to predict %DC and %D*COD* accurately and the stability of the process in time, the output of the reaction was monitored during 90 min at the optimum conditions of pH = 3, H_2O_2 = 24.3 mM and *SZVI* = 2000 mg/L to a final %DC 95% and %D*COD* of 76%. Fig. 2 depicts the evolution of color, *COD* and *TOC* as a function of reaction time during the treatment process. As shown in Fig. 3, there was a fast oxidation during the first 60 min of reaction; then the removal of color, COD and TOC remained constant, this is because iron species are continuously released to the aqueous phase in the SZVI/H_2O_2 process, but the H_2O_2 is a limit reagent, as shown in Eqs ((2) and (3)); therefore, when H_2O_2 is depleted, the reaction stabilizes. The color removal was faster than the *COD* and *TOC* removals, this suggests that chromophoric groups were quickly broken by the oxidation process. Based on the previously presented results, it can be assumed that ITWW treatment occurred in 2 steps, first is decolorization and the second involves further decomposition of by-products. This can be indirectly confirmed by the COD and TOC measures during the reaction time (Fig. 2); which are in agreeance with the results reported in other studies (Lin et al., 2008; Dutta et al., 2016). After a reaction time of 60 min, the color of the sample vanished almost completely, and the dark blue wastewater gradually changed to light blue and finally became colorless.

After treatment, the *COD* decreased from 875 mgL^{-1} to 208 (<400 mgL^{-1}, the National Discharge Standard of Colombia) and the *TOC* decreased from 324 mgL^{-1} to 93 mgL^{-1}, this suggests that a great portion of the organic compounds was mineralized to CO_2 and another part degraded to lesser organic compounds. On the other hand, SZVI/H_2O_2 mechanism is explained by the chemical oxidation of the pollutants with •OH radicals that are especially efficient for the degradation of soluble compounds. Table 1 shows the physical chemical properties of ITWW before and after the treatment process. After SZVI/H_2O_2, TOC was reduced by 71% while BOD_5 is reduced by 53.6% implying that SZVI/H_2O_2 is efficient in removing a high portion of organic content. Turbidity removal was 98.6%, meaning that almost all suspended solids are removed from water by SZVI/H_2O_2. Also, BOD_5/COD of after process wastewater is 0.4; indicating that the biodegradability of this wastewater is high.

As can be seen in Fig. 2 (a), pH values increased with reaction time. This behavior may be attributed to the significant contribution of ZVI-mediated proton reduction under both reductive and oxidative conditions. H^+ ions were consumed in the course of reaction leading to the increase in pH value of solution (Eqs (1) and (2)). Similar behavior was reported in other investigations (Donadelli et al., 2018; Santos-juanes et al., 2017; He et al., 2013). Besides, the operational cost of the SZVI/H_2O_2 process is 1.04 USD/m^3, relatively reasonable and moderate value that is similar to others reported in previous works (reported operational cost ranges between 0.50 USD/m^3 and 14.50 USD/m^3) (GilPavas et al., 2017; GilPavas et al., 2018).

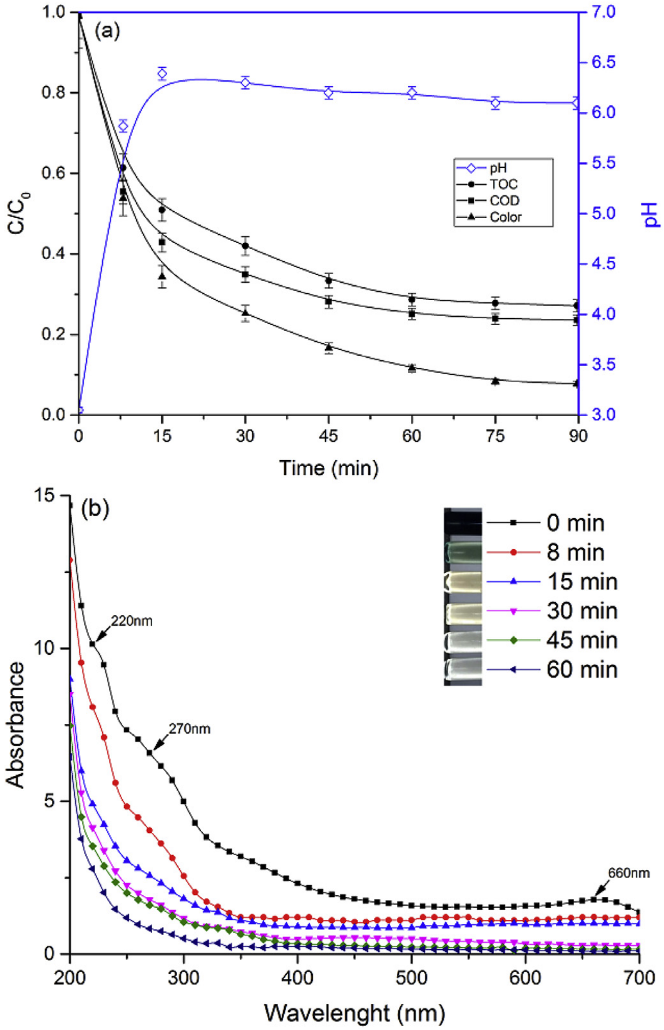

Fig. 2. (a) The transformation of the color, COD and TOC removal in wastewater during the SZVI/H_2O_2 process. Experimental conditions: pH = 3, H_2O_2 concentration 24.3 mM, SZVI dosage = 2000 mg/L, 500 rpm, and 90 min of reaction time. (b) UV-vis absorption spectrum. (For interpretation of the references to color in this figure legend, the reader is referred to the Web version of this article.)

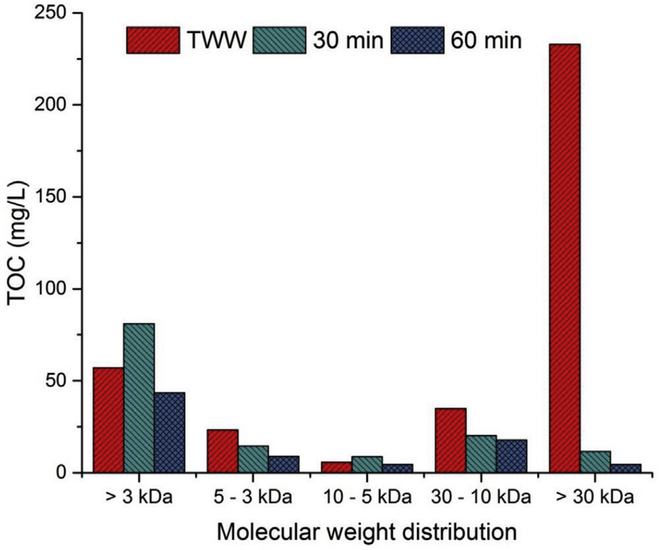

Fig. 3. Molecular weight distribution of the sample before and after 30 and 60 min of SZVI/H_2O_2 process.

The textile wastewater was also treated by the homogeneous Fenton process. The operational conditions for the homogeneous Fenton process were optimized by BBD and RSM ($Fe^{2+} = 1$ mM, $H_2O_2 = 21$ mM and pH = 3), at such conditions, after 90 min of reaction, the process led to color, COD and TOC reductions of 90%, 74% and 62% respectively (as shown in Fig. S2 and Table S1). Additionally, biodegradability (BOD_5/COD) increased from 0.2167 to 0.41. Likewise, the toxicity also decreased from 60% to 20%. Also, it was found that there is less sludge formation in the SZVI/H_2O_2 process (0.295 kg/m^3) than in the homogeneous Fenton Process (0.496 kg/m^3). On the other hand, the cost was found to be around 2.1 USD/m^3, which is a greater than cost of SZVI process reported in this research work. It was found that SZVI/H_2O_2 process is more efficient and economic than homogeneous Fenton process for color, COD and TOC removal. From this result it seems that SZVI/H_2O_2 process is a good alternative for removal of color, COD and TOC from textile wastewater. The process was also evaluated with H_2O_2 alone and SZVI alone. The percentage of degradation of COD was 26% and 5% respectively (as shown in Fig. S3). It was clearly observed that individual systems (SZVI and H_2O_2) were ineffective since they need an activator for the generation of •OH radical to attack organic components.

3.7. *Evaluation of after process compounds*

To analyze the evolution of contaminants during the SZVI/H_2O_2 process, organic contaminants in the sample were characterized before and after the process using molecular weight distribution (MWD) measurement, ultraviolet-visible (UV–Vis), HPLC analysis, biodegradability and toxicity. Control runs with H_2O_2 and SZVI were also performed during this stage; a run of TWW with only SZVI yielded a %DDQO of 10% after 60 min, while the one with only H_2O_2 had a %DDQO of 26% after the same time, this suggests that, although SZVI load is not significant in the range that was evaluated, there is a significant synergistic effect of SZVI with H_2O_2.

MWD of organic compounds (TOC) in ITWW before and after the SZVI/H_2O_2 process was analyzed by a membrane separation method. The original sample was mainly composed of organic matter with high molecular weight (MW) while the after treatment sample was mostly composed of pollutants of low molecular weight (<3 kDa) as shown in Fig. 3.

As can be seen in Fig. 2 (b), the UV-vis spectrum of the ITWW sample (time = 0 min) consists primarily of three characteristic absorption bands: at 220 and 270 nm, associated to benzenic rings; and at 660 nm, referred to indigo dye. After 60 min of the process, the bands at 220 and 660 nm disappeared, and the sample was almost colorless. However, the band at 270 nm remained, and aromatic compounds removal is ca. 87%, indicating the formation of some intermediate degradation compounds. Some reaction intermediates like tartaric, formic, oxalic and fumaric acid can be formed because of the oxidation of the azo dyes, their formation is highly dependent on the initial dye concentration and some of them are more stable and toxic than their parent compounds (Kang et al., 2000).

Fig. 4 shows the concentration of carboxylic acids that were formed as by-products during the process. Ion-exclusion chromatograms of the sample during the process time showed the presence of peaks associated to short-chain linear carboxylic acids that were generated during the SZVI/H_2O_2 treatment of ITWW. Oxalic (tr = 7.2 min), tartaric (tr = 9.6 min), formic (tr = 14.9 min), acetic (tr = 15.8 min) and fumaric (tr = 16.1 min) acids were detected. Maleic acid is produced by the oxidation of the benzenic ring in aromatic byproducts, which are subsequently oxidized to oxalic, formic and tartaric acids (Oturan et al., 2008; Skoumal et al.,

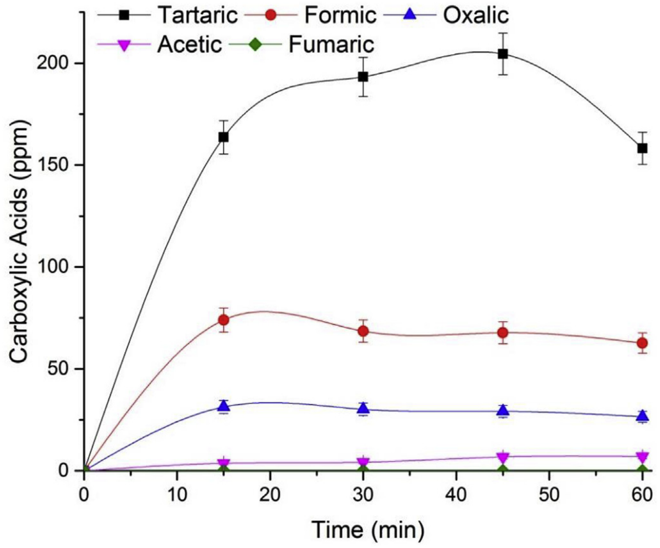

Fig. 4. Evolution of carboxylic acids generated during the degradation of ITWW by SZVI/H_2O_2 treatment at the same conditions of Fig. 2. Acid: (■) tartaric, (●) formic, (▲) oxalic, (▼) acetic and (◆) fumaric.

2008). Since tartaric, formic, oxalic and formic acids are ultimate carboxylic acids, they are likely to become into CO_2 after oxidation.

At the end of the treatment of the ITWW, 158.2 mg/L of tartaric acid, 62.7 mg/L of formic acid, 26.55 of oxalic acid and 6.98 of acetic acid were detected (see Fig. 4). That means that the pollutants in the sample are finally degraded to short-linear carboxylic acids.

Useful information can also be obtained from the carbon oxidation state (COS) and average oxidation state (AOS). The carbon oxidation state (COS) of the samples was calculated with Eq. (14), where TOC_0 is the TOC of the initial sample and COD is the chemical oxygen demand at the sampling time (expressed as mg/L). CO_2 generated by the organic oxidation (oxidation state 4+) is considered the highest oxidation state and is included in the calculation (Masiello et al., 2008). As presented in Fig. 5, there was a quick oxidation during the first 10 min of reaction; then the COS increased only slightly.

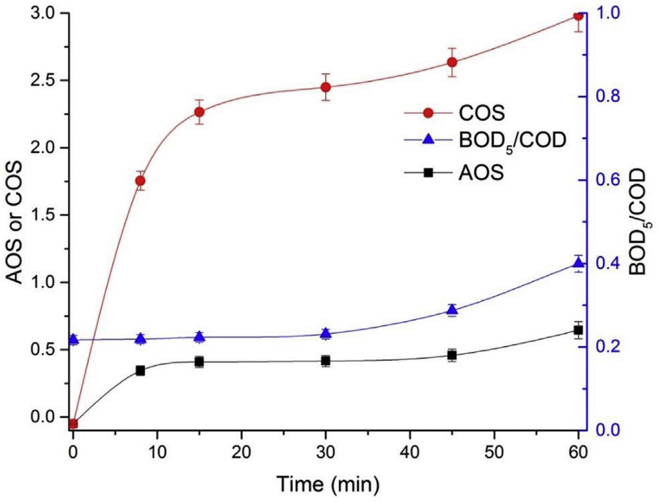

Fig. 5. Average oxidation state (AOS), carbon oxidation state (COS) and BOD_5/COD ratio along 60 min of SZVI/H_2O_2 treatment under the same conditions of Fig. 2.

$$COS = 4 - 1.5*\left(\frac{COD}{TOC_0}\right) \quad (14)$$

The average oxidation state (AOS) is used to reveal changes in the content of the sample that might lead to variations of the biodegradability/toxicity of the sample (GilPavas et al., 2018). The AOS was estimated by Eq. (15); this is similar to Eq. (14), but the TOC at the sampling time is used instead of the initial one, thus, only the remaining matter in the solution is considered in the calculation. Hence, AOS cannot be considered a measure of the process efficiency, but it shows variations in the composition of organic pollutants. Fig. 5 shows that AOS varies considerably during the first 10 min of reaction; thus, it seems important to measure toxicity/biodegradability of the sample.

$$AOS = 4 - 1.5*\left(\frac{COD}{TOC}\right) \quad (15)$$

As can be seen in Fig. 5, both AOS and COS increased during the reaction time, especially during the first 10 min of reaction, this is an indicator of the degradation of the complex organic pollutants into lesser molecules with a higher oxidation state.

The biodegradability index (BOD_5/COD) is usually used to assess if physicochemical processes are able to increase biodegradability and be used as pretreatment for the biological ones (Hsu et al., 2004). Fig. 5 shows its behavior during SZVI/H_2O_2 process. The BOD_5/COD of the ITWW sample was 0.2167 (Table 1), indicating a low biodegradability. This value increased up to 0.4 after the SZVI/H_2O_2 process. This suggests that the final effluent is likely biodegradable (BOD5/COD ratio ≥ 0.4).

As some byproducts of AOP's have been reported more toxic than their parent compounds (Kang et al., 2000), a toxicity assessment before and after the SZVI/H_2O_2 process was performed by checking on A. Salina's mortality in the samples. For the ITWW sample, 60% of mortality was found, while 20% was observed for the sample after the process. This suggests that, although some of the pollutants might be more toxic than the original ones, their concentration is such that the sample is less toxic than the original one. A control group, using deionized water and under the same experimental conditions, was also included for this assessment, which yielded a mortality of 0%; therefore, there is a low probability that the diminishing in mortality is attributed to effects different to the composition of the samples.

Moreover, the above information suggests that the sample after the SZVI/H_2O_2 is not only ready to be discharged, but an additional process could be considered so that it can be recirculated to the production process, this would help to make the process more viable due to the savings in process water (Prato-garcia & Vasquez-medrano, 2018). Due to the low concentration of complex organic pollutants and the low values in parameters such as TS, color and turbidity; additional processes like reverse osmosis (RO), ion exchange (IE) and ultrafiltration could be considered, as the equipment wouldn't be saturated quickly, and the operation cost might be competitive. Moreover, considering the biodegradability of the sample, the coupling of a biological treatment with the SZVI/H_2O_2 process could be considered for future studies (Soares et al., 2017; Trapido et al., 2017).

4. Conclusions

This work shows the capability of the SZVI/H_2O_2 process for the removal of organic contaminants present in a TWW effluent, characterized by its low biodegradability and high quantity of persistent compounds. The operational conditions for the SZVI/H_2O_2 process were optimized by BBD and RSM (SZVI = 2000 mg/L,

$H_2O_2 = 24.3$ mM and $pH = 3$), at such conditions, after 60 min of reaction, the process led to color, COD and TOC reductions of 95%, 76% and 71% respectively. Additionally, biodegradability (BOD_5/COD) increased from 0.2167 to 0.4 and toxicity decreased from 60% to 20%.

AOS and COS increased from −0.051 to 0.64 and 2.9 respectively; also, the molecular weight distribution showed that there was a significant decrease in the molecular weight of the pollutants after the process, this suggests that the post-process effluent is mainly polluted by short chain organic compounds, most likely carboxylic acids; this is also confirmed by the HPLC test performed, which showed concentrations of these acids that were equivalent to 76% of the TOC.

The sample characterization suggests that the process is effective enough for the effluent to be discharged and its cost was found to be around 1.04 USD/m^3, which is a lower cost than that of some of the processes reported in previous works. Moreover, as biodegradability increases, a coupled process with biological treatment could be considered to attain an even lower operational cost. Also, additional processes could be considered in order to recycle the water of this treatment.

Main finding

SZVI/H_2O_2 process at optimum conditions successfully degraded organic pollutants, complying with the regulation for discharge, increasing its biodegradability and reducing its toxicity.

Acknowledgements

The authors acknowledge the Research directorate of EAFIT University, Medellín, Colombia for providing the financial support for this research. The staff of the Process Engineering Laboratories are also recognized for their participation.

Appendix A. Supplementary data

Supplementary data to this article can be found online at https://doi.org/10.1016/j.envpol.2019.06.104.

References

American Public Health Association (APHA), 2012. American Water Works Association (AWWA), Water Environmental Federation (WEF), Standard Methods for the Examination of Water and Wastewater, twenty-second ed. Washington, D.C.

Badawy, M.I., Wahaab, R.A., El-Kalliny, A.S., 2009. Fenton-biological treatment processes for the removal of some pharmaceuticals from industrial wastewater. J. Hazard Mater. 167, 567–574. https://doi.org/10.1016/j.jhazmat.2009.01.023.

Bankole, P.O., Adekunle, A.A., Obidi, O.F., Olukanni, O.D., Govindwar, S.P., 2017. Journal of Environmental Chemical Engineering Degradation of indigo dye by a newly isolated yeast , Diutina rugosa from dye wastewater polluted soil. J. Environ. Chem. Eng. 5, 4639–4648. https://doi.org/10.1016/j.jece.2017.08.050.

Cao, J., Wei, L., Huang, Q., Wang, L., Han, S., 1999. Reducing degradation of azo dye by zero-valent iron in aqueous solution. Chemosphere 38, 565–571. https://doi.org/10.1016/S0045-6535(98)00201-X.

Chen, J.L., Al-Abed, S.R., Ryan, J.A., Li, Z., 2001. Effects of pH on dechlorination of trichloroethylene by zero-valent iron. J. Hazard Mater. 83, 243–254. https://doi.org/10.1016/S0304-3894(01)00193-5.

da Costa Filho, B.M., da Silva, V.M., Silva, J. de O., da Hora Machado, A.E., Trovó, A.G., 2016. Coupling coagulation, flocculation and decantation with photo-Fenton process for treatment of industrial wastewater containing fipronil: biodegradability and toxicity assessment. J. Environ. Manag. 174, 71–78. https://doi.org/10.1016/j.jenvman.2016.03.019.

Donadelli, J.A., Carlos, L., Arques, A., García, F.S., 2018. Environmental Kinetic and mechanistic analysis of azo dyes decolorization by ZVI-assisted Fenton systems : pH-dependent shift in the contributions of reductive and oxidative transformation pathways. Appl. Catal. B Environ. 231, 51–61. https://doi.org/10.1016/j.apcatb.2018.02.057.

Dutta, S., Saha, R., Kalita, H., Bezbaruah, A.N., 2016. Rapid reductive degradation of azo and anthraquinone dyes by nanoscale zero-valent iron. Environ. Technol. Innovat. 5, 176–187. https://doi.org/10.1016/j.eti.2016.03.001.

N.P.V., Gandhimathi, R., Thanga Ramesh, S., 2013. Degradation of dyes from aqueous solution by fenton processes: a review. Environ. Sci. Pollut. Res. 20, 2099–2132. https://doi.org/10.1007/s11356-012-1385-z.

Garcia-segura, S., El-ghenymy, A., Centellas, F., Rodríguez, R.M., Arias, C., Garrido, J.A., Cabot, P.L., Brillas, E., 2012. Comparative degradation of the diazo dye Direct Yellow 4 by electro-Fenton , photoelectro-Fenton and photo-assisted electro-Fenton. J. Electroanal. Chem. 681, 36–43. https://doi.org/10.1016/j.jelechem.2012.06.002.

Ghanbari, F., Moradi, M., 2015. A comparative study of electrocoagulation, electrochemical Fenton, electro-Fenton and peroxi-coagulation for decolorization of real textile wastewater: electrical energy consumption and biodegradability improvement. J. Environ. Chem. Eng. 3, 499–506. https://doi.org/10.1016/j.jece.2014.12.018.

GilPavas, E., Dobrosz-Gómez, I., Gómez-García, M.Á., 2017. Coagulation-flocculation sequential with Fenton or Photo-Fenton processes as an alternative for the industrial textile wastewater treatment. J. Environ. Manag. 191, 189–197. https://doi.org/10.1016/j.jenvman.2017.01.015.

GilPavas, E., Arbeláez-Castaño, P., Medina, J., Acosta, D., 2017. Combined Electrocoagulation and Electro-Oxidation of Industrial Textile Wastewater Treatment in a Continuous Multi-Stage Reactor Electrocoagulation and Electro-Oxidation of Industrial Textile Wastewater Treatment. https://doi.org/10.2166/wst.2017.415.

GilPavas, E., Dobrosz-gómez, I., Gómez-garcía, M.Á., 2018. Optimization of sequential chemical coagulation - electro-oxidation process for the treatment of an industrial textile wastewater. J. Water Process Eng. 22, 73–79. https://doi.org/10.1016/j.jwpe.2018.01.005.

Guo, X., Yang, Z., Liu, H., Lv, X., Tu, Q., Ren, Q., Xia, X., Jing, C., 2015. Common oxidants activate the reactivity of zero-valent iron (ZVI) and hence remarkably enhance nitrate reduction from water. Separ. Purif. Technol. 146, 227–234. https://doi.org/10.1016/j.seppur.2015.03.059.

He, Y., Gao, J., Feng, F., Liu, C., Peng, Y., Wang, S., 2012. The comparative study on the rapid decolorization of azo , anthraquinone and triphenylmethane dyes by zero-valent iron. Chem. Eng. J. 179, 8–18. https://doi.org/10.1016/j.cej.2011.05.107.

He, C., Yang, J., Zhu, L., Zhang, Q., Liao, W., Liu, S., Liao, Y., 2013. pH-dependent degradation of acid orange II by zero-valent iron in presence of oxygen. Separ. Purif. Technol. 117, 59–68. https://doi.org/10.1016/j.seppur.2013.04.028.

Hendaoui, K., Ayari, F., Ben, I., Ben, R., Darragi, F., 2018. Real indigo dyeing effluent decontamination using continuous electrocoagulation cell : study and optimization using Response Surface Methodology. Process Saf. Environ. Protect. 116, 578–589. https://doi.org/10.1016/j.psep.2018.03.007.

Hsu, Y., Yang, H., Chen, J., 2004. The enhancement of the biodegradability of phenolic solution using preozonation based on high ozone utilization, 56, 149–158. https://doi.org/10.1016/j.chemosphere.2004.02.011.

Kallel, M., Belaid, C., Boussahel, R., Ksibi, M., 2009. Olive Mill Wastewater Degradation by Fenton Oxidation with Zero-Valent Iron and Hydrogen Peroxide, vol. 163, pp. 550–554. https://doi.org/10.1016/j.jhazmat.2008.07.006.

Kang, S.F., Liao, C.H., Po, S.T., 2000. Decolorization of textile wastewater by photo-fenton oxidation technology. Chemosphere 41, 1287–1294. https://doi.org/10.1016/S0045-6535(99)00524-X.

Katsoyiannis, I.A., Ruettimann, T., Hug, S.J., 2008. pH dependence of fenton reagent generation and as(III) oxidation and removal by corrosion of zero valent iron in aerated water. Environ. Sci. Technol. 42, 7424–7430. https://doi.org/10.1021/es800649p.

Kavitha, V., Palanivelu, K., 2004. The role of ferrous ion in Fenton and photo-Fenton processes for the degradation of phenol. Chemosphere 55, 1235–1243. https://doi.org/10.1016/j.chemosphere.2003.12.022.

Kavitha, V., Palanivelu, K., 2005. Destruction of cresols by Fenton oxidation process. Water Res. 39, 3062–3072. https://doi.org/10.1016/j.watres.2005.05.011.

Keenan, C.R., Sedlak, D.L., 2008. Factors affecting the yield of oxidants from the reaction of nanoparticulate zero-valent iron and oxygen. Environ. Sci. Technol. 42, 1262–1267. https://doi.org/10.1021/es7025664.

Kumar, A., Jena, S., Acharya, B.C., Mishra, B.K., 2012. Removal of azo dye in innovative constructed wetlands : influence of iron scrap and sulfate reducing bacterial enrichment. Ecol. Eng. 49, 53–58. https://doi.org/10.1016/j.ecoleng.2012.08.032.

Lin, Y.T., Weng, C.-H., Chen, F.-Y., 2008. Effective removal of AB24 dye by nano/micro-size zero-valent iron. Separ. Purif. Technol. 64, 26–30. https://doi.org/10.1016/j.seppur.2008.08.012.

Masiello, C.A., Gallagher, M.E., Randerson, J.T., Deco, R.M., Chadwick, O.A., 2008. Evaluating two experimental approaches for measuring ecosystem carbon oxidation state and oxidative ratio. J. Geophys. Res. 0–9. https://doi.org/10.1029/2007JG000534.

Masomboon, N., Ratanatamskul, C., Lu, M.-C., 2009. Chemical oxidation of 2,6-dimethylaniline by electrochemically generated Fenton's reagent. J. Hazard Mater. 176, 92–98. https://doi.org/10.1016/j.jhazmat.2009.11.003.

Ming-Chin, C., Hung-Yee, S., Hsin-Hung, Y., Yi-Chun, S., 2006. Reductive decolourization and total organic carbon reduction of the diazo dye CI Acid Black 24 by zero-valent iron powder. J. Chem. Technol. Biotechnol. 81, 1259–1266. https://doi.org/10.1002/jctb.1543.

Montgomery, D.C., 2017. Design and Analysis of Experiments. John wiley & sons.

Olcay, T., Merve, Simseker, Isık, K., Tugba, Ö.-H., 2014. Abatements of reduced sulphur compounds, colour, and organic matter from indigo dyeing effluents by electrocoagulation. Environ. Technol. 1577–1588. https://doi.org/10.1080/09593330.2013.873824.

Oturan, M.A., Pimentel, M., Oturan, N., Sirés, I., 2008. Reaction sequence for the mineralization of the short-chain carboxylic acids usually formed upon cleavage of aromatics during electrochemical Fenton treatment. Electrochim. Acta 54, 173–182. https://doi.org/10.1016/j.electacta.2008.08.012.

Palma-goyes, R.E., Silva-agredo, J., González, I., Torres-palma, R.A., 2014. Comparative degradation of indigo carmine by electrochemical oxidation and advanced oxidation processes. Electrochim. Acta 140, 427–433. https://doi.org/10.1016/j.electacta.2014.06.096.

Prato-garcia, D., Vasquez-medrano, R., 2018. Photo-Fenton processes in raceway reactors : technical , economic , and environmental implications during treatment of colored wastewaters. J. Clean. Prod. 182, 818–829. https://doi.org/10.1016/j.jclepro.2018.02.058.

Santos-juanes, L., Einschlag, F.S.G., Amat, A.M., Arques, A., 2017. Combining ZVI reduction with photo-Fenton process for the removal of persistent pollutants. Chem. Eng. J. 310, 484–490. https://doi.org/10.1016/j.cej.2016.04.114.

Segura, Y., Martínez, F., Melero, J.A., Fierro, J.L.G., 2015. Zero valent iron (ZVI) mediated Fenton degradation of industrial wastewater : treatment performance and characterization of final composites. Chem. Eng. J. 269, 298–305. https://doi.org/10.1016/j.cej.2015.01.102.

Skoumal, M., Arias, C., Cabot, P., Centellas, F., Garrido Ponce, J.A., María Rodríguez, R., Brillas, E., 2008. Mineralization of the biocide chloroxylenol by electrochemical advanced oxidation processes. Chemosphere 71, 1728–1729. https://doi.org/10.1016/j.chemosphere.2007.12.029.

Soares, P.A., Souza, R., Soler, J., Silva, T.F.C.V., Guelli, S.M.A., Souza, U., Boaventura, R.A.R., Vilar, V.J.P., 2017. Remediation of a synthetic textile wastewater from polyester-cotton dyeing combining biological and photochemical oxidation processes. Separ. Purif. Technol. 172, 450–462. https://doi.org/10.1016/j.seppur.2016.08.036.

Trapido, M., Tenno, T., Goi, A., Dulova, N., Kattel, E., Klauson, D., Klein, K., Tenno, T., Viisimaa, M., 2017. Journal of Water Process Engineering Bio-recalcitrant pollutants removal from wastewater with combination of the Fenton treatment and biological oxidation. J. Water Process Eng. 16, 277–282. https://doi.org/10.1016/j.jwpe.2017.02.007.

Zhen, G., Lu, X., Li, Y., Liu, Y., Zhao, Y., 2015. Influence of zero valent scrap iron (ZVSI) supply on methane production from waste activated sludge. Chem. Eng. J. 263, 461–470. https://doi.org/10.1016/j.cej.2014.11.003.

Zhou, T., Lu, X., Wang, J., Wong, F., Li, Y., 2009. Rapid decolorization and mineralization of simulated textile wastewater in a heterogeneous Fenton like system with/without external energy, 165, 193–199. https://doi.org/10.1016/j.jhazmat.2008.09.100.